HHS Public Access

Author manuscript

Colloids Surf B Biointerfaces. Author manuscript; available in PMC 2020 January 01.

Published in final edited form as:

Colloids Surf B Biointerfaces. 2019 January 01; 173: 386–391. doi:10.1016/j.colsurfb.2018.09.080.

Incorporation of Functionalized Carbon Nanotubes into Hydrophobic Drug Crystals for Enhancing Aqueous Dissolution

Kun Chen[1] and **Somenath Mitra**[1,*]

[1]Department of Chemistry and Environmental Science, New Jersey Institute of Technology, Newark, NJ 07102, USA

Abstract

We present for the first time the direct incorporation of carboxylated carbon nanotubes (f-CNTs) into hydrophobic drug particles during their formation via anti-solvent precipitation. The approach was tested using two drugs namely antifungal agent Griseofulvin (GF) and antibiotic Sulfamethoxazole (SMZ) that had very different aqueous solubility. It was observed that the f-CNTs dispersed in the water served as nucleating sites for crystallization and were readily incorporated into the drug particles without altering crystal structure or other properties. The results showed that the hydrophilic f-CNTs dramatically enhanced dissolution rate for both drugs, and the time necessary to reach 80% dissolution (t_{80}) reduced from 67 to 10 with the incorporation of 5.1% f-CNTs in SMZ, and from 66 to 18 min with 4.0% f-CNTs in GF. The enhanced dissolution is attributed to the fact that the hydrophilic f-CNTs served as conduits for bringing in water in close contact with the drug crystals.

Graphical Abstract

*Corresponding author. Somenath.Mitra@njit.edu (Somenath Mitra).

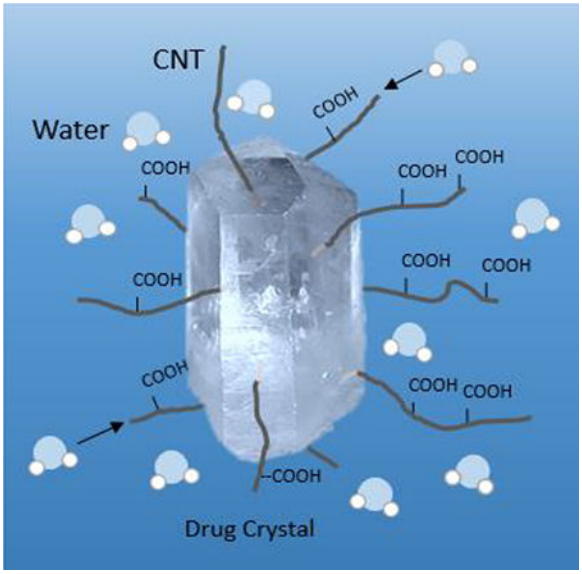

Keywords

Hydrophobic drugs; drug delivery; bioavailability; carbon nanotubes; dissolution rate; nanomedicine

1. INTRODUCTION

The high aspect ratio, potential for unique functionalization via covalent and non-covalent means have made carbon nanotubes (CNTs) attractive in many medical, therapeutic and nano medicine applications [1]. The CNTs have demonstrated excellent potential in tissue engineering, scaffolding, as material for bone, neuron and cell growth, thermal ablation and photo-thermal therapy, and as materials that promote differentiation of stem cells into specific lineages [2–14]. They have been used to deliver a wide range of small molecules such as chemotherapeutic drugs [15–21], anti-inflammatory and antimicrobials agents [22–23], and as carriers for controlled release [24]. They have also been used to deliver complex molecules such as peptide based vaccines [25–26], antibodies [27], nucleic acids proteins and genes [28]. CNTs have been particularly attractive in targeted delivery because they have shown enhanced permeability and retention in tumor tissues, their needle-like shape can facilitate transmembrane penetration and they have been shown to enter cells via endocytosis [29].

Drug loadings on CNTs have been addressed via covalent and noncovalent functionalization. Functionalization by a hydrophilic group also improves aqueous dispensability and reduces cytotoxicity [30–31]. Varieties of small and large molecules have been covalently attached to CNTs and it remains a popular approach to drug loading [32]. Besides direct conjugation of the active molecule, functionalization of CNTs with carboxylic, amine and polymer molecules have been used to facilitate the physical adsorption of drugs on CNTs surface. Non-covalent coating of CNTs for the purpose of drug delivery include amphiphilic macromolecules like lipid and polymers [32], cancer drug [33–34] and anti-Alzheimer drug [35]. CNTs have also been used for controlled release. For example, drugs encapsulated into

oxidized CNTs with the open ends capped with thiol modified gold nanoparticles have shown controlled release activity [36], Heparin attachment to carbodiimide functionalized CNTs have shown prolonged anticoagulant activity [37], a dual-targeted drug carrier for prolonged release has been designed by combining CNTs with folic acid and iron nanoparticles [38]. Electrical properties of CNTs have been utilized to design hydrogel systems to electro-responsive drug release [39], and nano precipitation technique has been reported where water soluble drugs have been incubated with CNTs followed by solvent evaporation where the drug adsorbed in the interstitial spaces in the CNTs to show slow release [24]. While there is much ongoing effort for using CNTs in drug delivery and biomedical applications, it is worth noting that there have been concerns about the toxicity of CNTs and numerous in vitro and in vivo studies have been carried out with conflicting reports [40–48]. However, functionalization with carboxyl group has shown to be an effective way to mitigate MWCNTs toxicity [49–50].

However, a large number of pharmaceutically active molecules have low aqueous solubility, reduced dissolution rate and these lead to poor absorption and therapeutic failures [51–52] of oral drugs. The inability to hydrogen bond in an aqueous medium is among the main reasons behind low aqueous solubility [53]. Biopharmaceutical classification system (BCS) highlights the fact that dissolution as a rate-limiting step for oral absorption of BCS class 2 and class 4 drugs, which have low solubility. About 70% of active pharmaceutical ingredients and new chemical entities are considered as poorly soluble which is great obstacle for drug development [54]. Increasing solubility can not only improve drug absorption but also potentially reduces dosage needed to achieve the same therapeutic effect while reducing side effects. Typically, dissolution can be improved by size reduction or incorporating into drug carriers [55]. Methods such as dry and wet milling and homogenization are conventional methods for the synthesis of micron/nano-scale drug particles where the control of particle size, morphology, and surface properties can be relatively challenging [55]. Precipitation processes are also effective methods for synthesizing micron and submicron hydrophobic drug particles [56]

Anti-solvent crystallization is a functionally simple and rapid precipitation process [57] where a drug is dissolved in a solvent and then contacted with a miscible anti-solvent to precipitate micro/nano particles. The physio-chemical properties of the anti-solvent can alter the rate of nucleation, crystal growth and colloidal behavior of the crystallizing molecule [57]. In the case of hydrophobic molecules, water which has relatively high miscibility with many polar solvents can serves as an anti-solvent [57]. Ultra-sonication is known to bring about uniform nucleation, rapid crystallization. Narrow size distribution can be obtained by carrying out the process in the presence of additives that prevent agglomeration [58].

An interesting possibility in anti-solvent precipitation is that the drug particles can also be directly incorporated into a drug delivery vehicle such as CNTs. Carboxylated CNTs which are highly water dispersible offer the potential to serve as nucleating sites for a hydrophobic drug during its anti-solvent synthesis. This could be a way to incorporate CNTs into the drug structure where some specific sites on the CNTs may provide targeting capabilities. Also, the hydrophilic CNTs incorporated into a hydrophobic drug could potentially enhance hydrogen bonding with the aqueous medium leading to faster dissolution. The objective of

this work was to study the possibility of incorporation of hydrophilic CNTs during anti-solvent synthesis of micron-scale drug particles and see if the CNTs would enhance dissolution. Of particular interest to this study were antifungal agent Griseofulvin (GF) and antibiotic Sulfamethoxazole (SMZ).

2. MATERIALS and METHODS

2.1 Materials

Griseofulvin (GF) and Sulfamethoxazole (SMZ) were purchased from Sigma Aldrich, USA. Sodium dodecyl sulphate (SDS) was purchased from GFS Chemicals. Hydrochloride acid was purchased from Fisher Sci. Raw multiwall carbon nanotube (20–30 nm diameter, 10–30 μm length) was purchased from Cheap Tubes. The water used in the experiments was purified with a Milli-Q Plus system.

2.2 Preparation of carbon nanotube-drug composite

Carboxylated multiwall carbon nanotubes (f-CNTs) were synthesized following a previously published methodology [49, 59–60]. In short, pre-weighed amounts of purified CNTs were treated in a microwave reactor (Model: CEM Mars) with a mixture of concentrated H_2SO_4 and HNO_3 at 140°C for 20 min. This led to the formation of carboxylic groups on the CNTs surface leading to high aqueous dispensability. The f-CNTs were filtered through a 10μm membrane filter, washed with water to a neutral pH and dried under vacuum at 80°C to a constant weight.

Anti-solvent precipitation was carried out at room temperature. Acetone was used to dissolve GF and SMZ. f-CNTs was dispersed in water under ultrasonic agitation for 10 min to serve as the anti-solvent. Then the f-CNTs suspension was added dropwise into the drug solution under ultra-sonication. The solution turned cloudy indicating that the crystals were formed and these are referred to as GF-CNT and SMZ-CNT respectively. Ultrasonication was stopped after all f-CNTs suspension was added. The resulting suspension was filtered and washed with water through a 10μm membrane filter. The filtered solid was collected and dried in a vacuum oven to a constant weight.

The resulting drug/CNTs composites were characterized with SEM, TEM, DSC, XRD and the release behavior was examined by dissolution testing. TGA was performed with PerkinElmer Pyris 1 thermogravimetric analyzer. Samples were heated from 30 to 1200°C under a 10ml/min air flow at 10°C per min. SEM was performed with LEO 1530VP. Samples were mounted on aluminum stubs with adhesive tape and coated with carbon using Quorrum EMS 150T ES sputtering coater to improve conductivity. Raman spectroscopy was carried out with DXR Raman Microscope from Thermo Scientific with 532 nm filter. XRD was carried out with PANalytical EMPYREAN XRD. Melting point was measured with PerkinElmer DSC 6000.

Dissolution measurements were carried out based on standard US Pharmacopeia Method (USP 41) with Symphony 7100 dissolution system. Since GF is absorbed in the lower intestine and SMZ in the stomach, the dissolution tests were carried out at different pH. For GF-CNT, the composite was added to 40mg/ml sodium dodecyl sulfate (pH 5.2) and stirred

at 75 rpm, 37°C. Samples were withdrawn at different points in time, filtered to remove CNTs and then analyzed with UV at 291 nm to determine the amount of GF dissolved. For SMZ-CNT samples, the composite was added in 0.1 N hydrochloric acid (pH 1.4) and stirred at 75 rpm at 37°C. Once again, the samples were withdrawn at different times, filtered and analyzed with UV at 265 nm to determine the amount of SMZ dissolved.

3. Results and Discussion

The aqueous solubility of Griseofulvin (GF) and Sulfamethoxazole (SMZ) were 12 μg/ml and 0.61 mg/ml respectively. It was possible to form excellent crystals of both these drugs in the presence of f-CNTs.

The SEM image of functionalized carbon nanotubes are shown on Figure 1 a. It shows that the structure of carbon nanotubes was not altered after microwave treatment. XRD spectra of f-CNTs is showed in Figure S-1 in supplemental materials. The RAMAN spectra of raw CNTs and f-CNTs are shown on Figure S-2 a and b in supplemental materials.

The amount of f-CNTs in the antisolvent was varied to make drug/CNT composites. The incorporated concentrations of f-CNTs in each composite were measured using TGA (Figure 2 a and b). The amount of f-CNTs incorporated in the GF crystals prepared from f-CNTs suspension containing 0.1, 0.5, 1.0, 2.0 and 5.0% were 2.3, 2.4, 2.7, 3.4 and 4.0% respectively. For SMZ-CNT, the corresponding values for the same f-CNTs suspensions were 1.3, 1.4, 2.5, 3.0 and 5.1% respectively. These are referred to as SMZ-CNT-X or GF-CNT-X where X represents the incorporation concentration of f-CNTs. Figure 1 b is a plot of incorporation concentration of f-CNTs in the drug as a function of f-CNTs in the original suspension. The f-CNTs served as nucleation point for drug crystallization.

The morphology of GF-CNT and SMZ-CNT samples was studied using SEM. Figure 3 a, b showed SEM images of pure GF and GF-CNT composites while Figure S-3 a, b in supplemental materials showed respective images of SMZ-CNT. The crystal shape and size did not depend on f-CNTs incorporation. All the samples showed the presence of the f-CNTs on the crystal surface. SEM of some samples are not presented here for brevity. The TEM images (Figures 4 a, b) clearly indicate that the f-CNTs were also embedded inside the drug crystals, the tubes were partially incorporated into the crystal while some portion remained outside. The section remaining outside was effective in increasing the composite's interactions with the aqueous phase during dissolution studies.

Figure 5 showed the RAMAN spectra of pure GF and GF-CNTs of various composition. The D-band at 1350 cm^{-1} and G-band at 1580 cm^{-1} from the f-CNTs were overlaid with peaks from SMZ and GF. The GF spectra showed strong peaks in the region 1550–1800cm $^{-1}$ and 2800–3200 cm^{-1} which were attributed to the C=O stretching of benzo furan ring and C-H stretching of GF respectively[61]. The same characteristic peaks were also observed in all samples, which indicated that the presence of the f-CNTs didn't change the chemical structure of GF. The similar observation was found in Figure S-4 in supplemental materials which showed RAMAN spectra of pure SMZ and SMZ-CNTs of various f-CNTs concentration.

XRD was used to study the crystal structure of the GF-CNT and SMZ-CNT composites. The scanning range for GF was 5 to 70 degrees and 5 to 50 degrees for SMZ. Figure 6 shows XRD spectra of pure GF, GF-CNT-2.7, GF-CNT-4.0. It was seen that the crystal structure did not change in the presence of f-CNTs. The spectra of pure drug and drug-CNTs composites were identical, and neither splitting nor shifting of the peak was observed for the drug-CNTs composites. This indicated that there was no change in polymorphism, which is an important consideration in drug synthesis. The similar observation was found in Figure S-5 in supplemental materials which showed XRD spectra of pure SMZ, SMZ-CNT-2.5 and SMZ-CNT-5.1.

The melting point were analyzed by DSC where the SMZ-CNT samples were heated from 25°C to 200°C, and GF was heated from 25°C to 250°C. Both samples were programed to cool down and reheated for the second time. The results are presented in Table 1. No significant change in melting point was observed between pure GF, SMZ and their respective composites with different f-CNTs concentrations indicating the drug structure weren't altered with incorporation of f-CNTs.

Dissolution Studies

Dissolution profiles for SMZ-CNT and GF-CNT are presented in Figure 7. It is evident from both profiles that the f-CNTs helped enhance the release of the drugs. It also showed that increasing concentration of f-CNTs in the composite increased the release rate quite dramatically. Table 1 shows the t_{50} and t_{80}, or the time necessary to reach 50 and 80% dissolution. Both t_{50} and t_{80} reduced with the increased concentration of f-CNTs. With the incorporation of 1.4% f-CNTs, the t_{50} and t_{80} of SMZ dropped from 22 to 10 min and from 67 to 29 min respectively. Corresponding drop for GF with 2.4% CNT incorporation were from 27 to 12 min and from 66 to 48 min respectively. Simple mixtures of the drugs with 5% f-CNTs were prepared and dissolution data are shown in Figure 7. The results showed that simply adding f-CNTs to the drug did not improve the dissolution. This demonstrated that the enhanced dissolution was brought about by incorporation into the crystal structure. The mediums used in the dissolution of both drugs are considered resemble to gastrointestinal environment, thus the dissolution behavior is relevant to human biology.

The increased dissolution was attributed to the two factors. The carboxylated CNTs were hydrophilic and hydrogen bonded well with water molecules and brought the latter into close contract with the drug crystals. The TEM image in Figure 4 shows that some f-CNTs were incorporated into the crystals. A water molecule could potentially adsorb on the hydrophilic f-CNTs and use it as a conduit to enter the crystal thus enhancing the dissolution.

4. Conclusion

The f-CNTs dispersed in the water served as nucleating sites for crystallization and were readily incorporated into both GF and SMZ during their formation via anti-solvent precipitation. The SEM and TEM images show f-CNTs incorporation and their presence inside as well as outside the crystals. Raman, XRD and DSC showed presence of f-CNTs didn't change the crystal structure and melting point with the incorporation of as much as

5.1% f-CNTs by weight. The increase in dissolution rate was dramatic with t_{50} and t_{80} reducing by 78 for and 73% respectively for GF, and the corresponding increase for SMZ were 77 and 85%. This paper presents a novel approach to f-CNTs incorporation that can go beyond enhancing dissolution and opens the door to targeting and other forms of drug delivery.

Supplementary Material

Refer to Web version on PubMed Central for supplementary material.

Acknowledgements

This work was funded by a grant from the National Institute of Environmental Health Sciences (NIEHS) under Grant No. R01ES023209. Any opinions, findings, and conclusions or recommendations expressed in this material are those of the author(s) and do not necessarily reflect the views of the NIEHS.

References

1. Klumpp C; Kostarelos K; Prato M; Bianco A, Functionalized carbon nanotubes as emerging nanovectors for the delivery of therapeutics. Biochimica et Biophysica Acta (BBA) - Biomembranes 2006, 1758 (3), 404–412. [PubMed: 16307724]
2. Harrison BS; Atala A, Carbon nanotube applications for tissue engineering. Biomaterials 2007, 28 (2), 344–353. [PubMed: 16934866]
3. Fabbro C; Ali-Boucetta H; Ros TD; Kostarelos K; Bianco A; Prato M, Targeting carbon nanotubes against cancer. Chemical Communications 2012, 48 (33), 3911–3926. [PubMed: 22428156]
4. Sitharaman B; Shi X; Walboomers XF; Liao H; Cuijpers V; Wilson LJ; Mikos AG; Jansen JA, In vivo biocompatibility of ultra-short single-walled carbon nanotube/biodegradable polymer nanocomposites for bone tissue engineering. Bone 2008, 43 (2), 362–370. [PubMed: 18541467]
5. Shi X; Sitharaman B; Pham QP; Liang F; Wu K; Edward Billups W; Wilson LJ; Mikos AG, Fabrication of porous ultra-short single-walled carbon nanotube nanocomposite scaffolds for bone tissue engineering. Biomaterials 2007, 28 (28), 4078–4090. [PubMed: 17576009]
6. Martinelli V; Cellot G; Toma FM; Long CS; Caldwell JH; Zentilin L; Giacca M; Turco A; Prato M; Ballerini L; Mestroni L, Carbon Nanotubes Promote Growth and Spontaneous Electrical Activity in Cultured Cardiac Myocytes. Nano Letters 2012, 12 (4), 1831–1838. [PubMed: 22432413]
7. Nayak TR; Jian L; Phua LC; Ho HK; Ren Y; Pastorin G, Thin Films of Functionalized Multiwalled Carbon Nanotubes as Suitable Scaffold Materials for Stem Cells Proliferation and Bone Formation. ACS Nano 2010, 4 (12), 7717–7725. [PubMed: 21117641]
8. Li X; Liu H; Niu X; Yu B; Fan Y; Feng Q; Cui F.-z.; Watari F, The use of carbon nanotubes to induce osteogenic differentiation of human adipose-derived MSCs in vitro and ectopic bone formation in vivo. Biomaterials 2012, 33 (19), 4818–4827. [PubMed: 22483242]
9. Moon HK; Lee SH; Choi HC, In Vivo Near-Infrared Mediated Tumor Destruction by Photothermal Effect of Carbon Nanotubes. ACS Nano 2009, 3 (11), 3707–3713. [PubMed: 19877694]
10. Zhou F; Wu S; Wu B; Chen WR; Xing D, Mitochondria-Targeting Single-Walled Carbon Nanotubes for Cancer Photothermal Therapy. Small 2011, 7 (19), 2727–2735. [PubMed: 21861293]
11. Zhou F; Wu S; Yuan Y; Chen WR; Xing D, Mitochondria-Targeting Photoacoustic Therapy Using Single-Walled Carbon Nanotubes. Small 2012, 8 (10), 1543–1550. [PubMed: 22422554]
12. Zhou F; Xing D; Ou Z; Wu B; Resasco DE; Chen WR, Cancer photothermal therapy in the near-infrared region by using single-walled carbon nanotubes. BIOMEDO 2009, 14 (2), 021009–021009-7.
13. Keefer EW; Botterman BR; Romero MI; Rossi AF; Gross GW, Carbon nanotube coating improves neuronal recordings. Nat Nano 2008, 3 (7), 434–439.

14. Lee HJ; Park J; Yoon OJ; Kim HW; Lee DY; Kim DH; Lee WB; Lee N-E; Bonventre JV; Kim SS, Amine-modified single-walled carbon nanotubes protect neurons from injury in a rat stroke model. Nat Nano 2011, 6 (2), 121–125.
15. Liu Z; Sun X; Nakayama-Ratchford N; Dai H, Supramolecular Chemistry on Water-Soluble Carbon Nanotubes for Drug Loading and Delivery. ACS Nano 2007, 1 (1), 50–56. [PubMed: 19203129]
16. Feazell RP; Nakayama-Ratchford N; Dai H; Lippard SJ, Soluble Single-Walled Carbon Nanotubes as Longboat Delivery Systems for Platinum(IV) Anticancer Drug Design. Journal of the American Chemical Society 2007, 129 (27), 8438–8439. [PubMed: 17569542]
17. Liu Z; Chen K; Davis C; Sherlock S; Cao Q; Chen X; Dai H, Drug Delivery with Carbon Nanotubes for In vivo Cancer Treatment. Cancer Research 2008, 68 (16), 6652–6660. [PubMed: 18701489]
18. Yang D; Yang F; Hu J; Long J; Wang C; Fu D; Ni Q, Hydrophilic multiwalled carbon nanotubes decorated with magnetite nanoparticles as lymphatic targeted drug delivery vehicles. Chemical Communications 2009, (29), 4447–4449. [PubMed: 19597621]
19. Pastorin G; Wu W; Wieckowski S; Briand JP; Kostarelos K; Prato M; Bianco A, Double functionalisation of carbon nanotubes for multimodal drug delivery. Chemical Communications 2006, (11), 1182–1184. [PubMed: 16518484]
20. Li J; Yap SQ; Chin CF; Tian Q; Yoong SL; Pastorin G; Ang WH, Platinum(iv) prodrugs entrapped within multiwalled carbon nanotubes: Selective release by chemical reduction and hydrophobicity reversal. Chem. Sci 2012, 3 (6), 2083–2087.
21. Ali-Boucetta H; Al-Jamal KT; McCarthy D; Prato M; Bianco A; Kostarelos K, Multiwalled carbon nanotube-doxorubicin supramolecular complexes for cancer therapeutics. Chemical Communications 2008, 8 (4), 459–461.
22. Benincasa M; Pacor S; Wu W; Prato M; Bianco A; Gennaro R, Antifungal Activity of Amphotericin B Conjugated to Carbon Nanotubes. ACS Nano 2011, 5 (1), 199–208. [PubMed: 21141979]
23. Wu W; Wieckowski S; Pastorin G; Benincasa M; Klumpp C; Briand J-P; Gennaro R; Prato M; Bianco A, Targeted Delivery of Amphotericin B to Cells by Using Functionalized Carbon Nanotubes. Angewandte Chemie International Edition 2005, 44 (39), 6358–6362. [PubMed: 16138384]
24. Shah M; Agrawal Y, Carbon Nanotube: A Novel Carrier for Sustained Release Formulation. Fullerenes, Nanotubes and Carbon Nanostructures 2012, 20 (8), 696–708.
25. Pantarotto D; Partidos CD; Hoebeke J; Brown F; Kramer E; Briand J-P; Muller S; Prato M; Bianco A, Immunization with Peptide-Functionalized Carbon Nanotubes Enhances Virus-Specific Neutralizing Antibody Responses. Chemistry & Biology 2003, 10 (10), 961–966. [PubMed: 14583262]
26. Pantarotto D; Partidos CD; Graff R; Hoebeke J; Briand J-P; Prato M; Bianco A, Synthesis, Structural Characterization, and Immunological Properties of Carbon Nanotubes Functionalized with Peptides. Journal of the American Chemical Society 2003, 125 (20), 6160–6164. [PubMed: 12785847]
27. McDevitt MR; Chattopadhyay D; Kappel BJ; Jaggi JS; Schiffman SR; Antczak C; Njardarson JT; Brentjens R; Scheinberg DA, Tumor Targeting with Antibody-Functionalized, Radiolabeled Carbon Nanotubes. Journal of Nuclear Medicine 2007, 48 (7), 1180–1189. [PubMed: 17607040]
28. Podesta JE; Al-Jamal KT; Herrero MA; Tian B; Ali-Boucetta H; Hegde V; Bianco A; Prato M; Kostarelos K, Antitumor activity and prolonged survival by carbon-nanotube-mediated therapeutic sirna silencing in a human lung xenograft model. Small 2009, 5 (10), 1176–1185. [PubMed: 19306454]
29. Lacerda L; Russier J; Pastorin G; Herrero MA; Venturelli E; Dumortier H; Al-Jamal KT; Prato M; Kostarelos K; Bianco A, Translocation mechanisms of chemically functionalised carbon nanotubes across plasma membranes. Biomaterials 2012, 33 (11), 3334–3343. [PubMed: 22289266]
30. Charbgoo F; Behmanesh M; Nikkhah M, Enhanced reduction of single-wall carbon nanotube cytotoxicity in vitro: Applying a novel method of arginine functionalization. Biotechnology and Applied Biochemistry 2015, 62 (5), 598–605. [PubMed: 25347997]

31. Mallakpour S; Zadehnazari A, Effect of amino acid-functionalization on the interfacial adhesion and behavior of multi-walled carbon nanotubes/poly(amide-imide) nanocomposites containing thiazole side unit. Journal of Polymer Research 2013, 20 (7), 1–12.
32. Tan JM; Arulselvan P; Fakurazi S; Ithnin H; Hussein MZ, A Review on Characterizations and Biocompatibility of Functionalized Carbon Nanotubes in Drug Delivery Design. Journal of Nanomaterials 2014, 2014, 20.
33. Milosavljevic V; Krejcova L; Guran R; Buchtelova H; Wawrzak D; Richtera L; Heger Z; Kopel P; Adam V, Exceptional release kinetics and cytotoxic selectivity of oxidised MWCNTs double-functionalised with doxorubicin and prostate-homing peptide. Colloids and Surfaces B: Biointerfaces 2017, 156, 123–132. [PubMed: 28527356]
34. Kumar M; Sharma G; Misra C; Kumar R; Singh B; Katare OP; Raza K, N-desmethyl tamoxifen and quercetin-loaded multiwalled CNTs: A synergistic approach to overcome MDR in cancer cells. Materials Science and Engineering: C 2018, 89, 274–282. 35. [PubMed: 29752099]
35. Lohan S; Raza K; Mehta SK; Bhatti GK; Saini S; Singh B, Anti-Alzheimer's potential of berberine using surface decorated multi-walled carbon nanotubes: A preclinical evidence. International Journal of Pharmaceutics 2017, 530 (1), 263–278. 36. [PubMed: 28774853]
36. Li J; Yap SQ; Yoong SL; Nayak TR; Chandra GW; Ang WH; Panczyk T; Ramaprabhu S; Vashist SK; Sheu F-S; Tan A; Pastorin G, Carbon nanotube bottles for incorporation, release and enhanced cytotoxic effect of cisplatin. Carbon 2012, 50 (4), 1625–1634.
37. Park T-J; Kim YS; Hwang T; Govindaiah P; Choi S-W; Kim E; Won K; Lee SH; Kim JH, Preparation and characterization of heparinized multi-walled carbon nanotubes. Process Biochemistry 2012, 47 (1), 113–118.
38. Li R; Wu R a.; Zhao L; Hu Z; Guo S; Pan X; Zou H, Folate and iron difunctionalized multiwall carbon nanotubes as dual-targeted drug nanocarrier to cancer cells. Carbon 2011, 49 (5), 1797–1805.
39. Spizzirri UG; Hampel S; Cirillo G; Nicoletta FP; Hassan A; Vittorio O; Picci N; Iemma F, Spherical gelatin/CNTs hybrid microgels as electro-responsive drug delivery systems. International Journal of Pharmaceutics 2013, 448 (1), 115–122. [PubMed: 23524119]
40. Liu X; Gurel V; Morris D; Murray DW; Zhitkovich A; Kane AB; Hurt RH, Bioavailability of Nickel in Single-Wall Carbon Nanotubes. Advanced Materials 2007, 19 (19), 2790–2796.
41. Poland CA; Duffin R; Kinloch I; Maynard A; Wallace WAH; Seaton A; Stone V; Brown S; MacNee W; Donaldson K, Carbon nanotubes introduced into the abdominal cavity of mice show asbestos-like pathogenicity in a pilot study. Nature Nanotechnology 2008, 3, 423.
42. Sato Y; Yokoyama A; Shibata K.-i.; Akimoto Y; Ogino S.-i.; Nodasaka Y;Kohgo T; Tamura K; Akasaka T; Uo M; Motomiya K; Jeyadevan B; Ishiguro M; Hatakeyama R; Watari F; Tohji K, Influence of length on cytotoxicity of multi-walled carbon nanotubes against human acute monocytic leukemia cell line THP-1 in vitro and subcutaneous tissue of rats in vivo. Molecular BioSystems 2005, 1 (2), 176–182. [PubMed: 16880981]
43. Jia G; Wang H; Yan L; Wang X; Pei R; Yan T; Zhao Y; Guo X, Cytotoxicity of Carbon Nanomaterials: Single-Wall Nanotube, Multi-Wall Nanotube, and Fullerene. Environmental Science & Technology 2005, 39 (5), 1378–1383. [PubMed: 15787380]
44. Pacurari M; Yin XJ; Zhao J; Ding M; Leonard SS; Schwegler-Berry D; Ducatman BS; Sbarra D; Hoover MD; Castranova V; Vallyathan V, Raw single-wall carbon nanotubes induce oxidative stress and activate MAPKs, AP-1, NF-kappaB, and Akt in normal and malignant human mesothelial cells. Environmental health perspectives 2008, 116 (9), 1211–7. [PubMed: 18795165]
45. Wang L; Luanpitpong S; Castranova V; Tse W; Lu Y; Pongrakhananon V; Rojanasakul Y, Carbon Nanotubes Induce Malignant Transformation and Tumorigenesis of Human Lung Epithelial Cells. Nano Letters 2011, 11 (7), 2796–2803. [PubMed: 21657258]
46. Pulskamp K; Diabaté S; Krug HF, Carbon nanotubes show no sign of acute toxicity but induce intracellular reactive oxygen species in dependence on contaminants. Toxicology Letters 2007, 168 (1), 58–74. [PubMed: 17141434]
47. Kagan VE; Konduru NV; Feng W; Allen BL; Conroy J; Volkov Y; Vlasova II; Belikova NA; Yanamala N; Kapralov A; Tyurina YY; Shi J; Kisin ER; Murray AR; Franks J; Stolz D; Gou P;

Klein-Seetharaman J; Fadeel B; Star A; Shvedova AA, Carbon nanotubes degraded by neutrophil myeloperoxidase induce less pulmonary inflammation. Nature Nanotechnology 2010, 5, 354.

48. Takagi D; Homma Y; Hibino H; Suzuki S; Kobayashi Y, Single-Walled Carbon Nanotube Growth from Highly Activated Metal Nanoparticles. Nano Letters 2006, 6 (12), 2642–2645. [PubMed: 17163681]
49. Wu Z; Wang Z; Yu F; Thakkar M; Mitra S, Variation in chemical, colloidal and electrochemical properties of carbon nanotubes with the degree of carboxylation. Journal of Nanoparticle Research 2017, 19 (1), 16. [PubMed: 29046611]
50. Allegri M; Perivoliotis DK; Bianchi MG; Chiu M; Pagliaro A; Koklioti MA; Trompeta A-FA; Bergamaschi E; Bussolati O; Charitidis CA, Toxicity determinants of multi-walled carbon nanotubes: The relationship between functionalization and agglomeration. Toxicology Reports 2016, 3, 230–243. [PubMed: 28959543]
51. Thorat AA; Dalvi SV, Liquid antisolvent precipitation and stabilization of nanoparticles of poorly water soluble drugs in aqueous suspensions: Recent developments and future perspective. Chemical Engineering Journal 2012, 181–182, 1–34.
52. Gao Y; Li LB; Zhai G, Preparation and characterization of Pluronic/TPGS mixed micelles for solubilization of camptothecin. Colloids and Surfaces B: Biointerfaces 2008, 64 (2), 194–199. [PubMed: 18325744]
53. Kipp JE, The role of solid nanoparticle technology in the parenteral delivery of poorly water-soluble drugs. International Journal of Pharmaceutics 2004, 284 (1–2), 109–122. [PubMed: 15454302]
54. Singh D; Bedi N; Tiwary AK, Enhancing solubility of poorly aqueous soluble drugs: critical appraisal of techniques. Journal of Pharmaceutical Investigation 2017.
55. Wong SM; Kellaway IW; Murdan S, Enhancement of the dissolution rate and oral absorption of a poorly water soluble drug by formation of surfactant-containing microparticles. International Journal of Pharmaceutics 2006, 317 (1), 61–68. [PubMed: 16647232]
56. Kakran M; Sahoo NG; Tan IL; Li L, Preparation of nanoparticles of poorly water-soluble antioxidant curcumin by antisolvent precipitation methods. Journal of Nanoparticle Research 2012, 14 (3), 757.
57. Lonare AA; Patel SR, Antisolvent Crystallization of Poorly Water Soluble Drugs. International Journal of Chemical Engineering and Applications 2013, 4 (5), 337–341.
58. Chan H-K; Kwok PCL, Production methods for nanodrug particles using the bottom-up approach. Advanced Drug Delivery Reviews 2011, 63 (6), 406–416. [PubMed: 21457742]
59. Wang Z; Wu Z; Di Benedetto G; Zunino Iii JL; Mitra S, Microwave synthesis of highly oxidized and defective carbon nanotubes for enhancing the performance of supercapacitors. Carbon 2015, 91, 103–113.
60. Wu Z; Hamilton RF; Wang Z; Holian A; Mitra S, Oxidation debris in microwave functionalized carbon nanotubes: Chemical and biological effects. Carbon 2014, 68 (Supplement C), 678–686.
61. Bolton BA; Prasad PN, Laser raman investigation of pharmaceutical solids: Griseofulvin and its solvates. Journal of Pharmaceutical Sciences 1981, 70 (7), 789–793. [PubMed: 7264929]

Highlights

- Hydrophilic, carboxylated carbon nanotubes were incorporated in drug crystals
- Crystal structure remained unchanged by incorporation via anti-solvent precipitation
- Hydrophilic carbon nanotubes dramatically enhanced dissolution of hydrophobic drugs

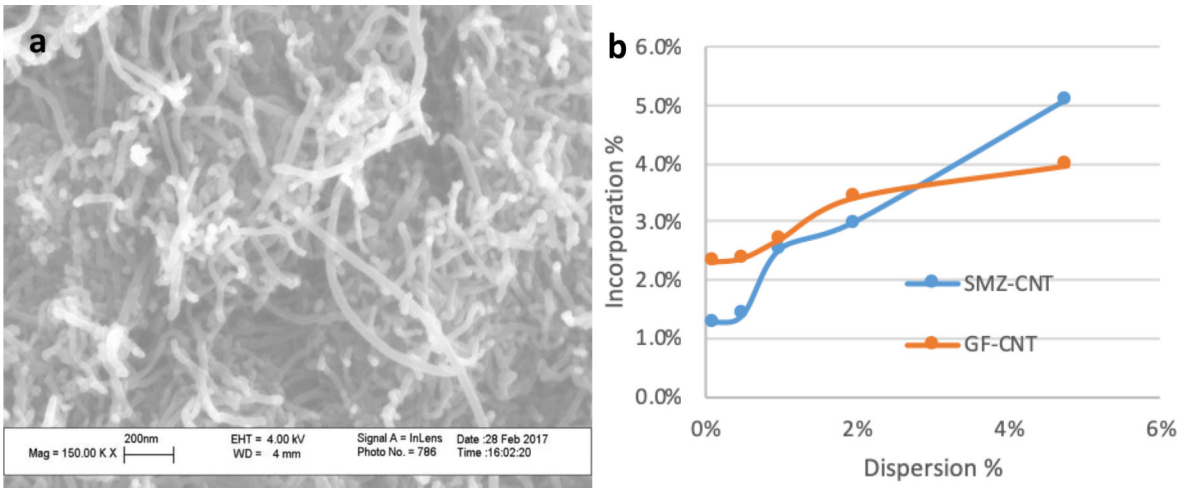

Figure 1.

(a) SEM image of f-CNTs, (b) Incorporation of CNTs in drug composites as a function of concentration of f-CNTs in the dispersion.

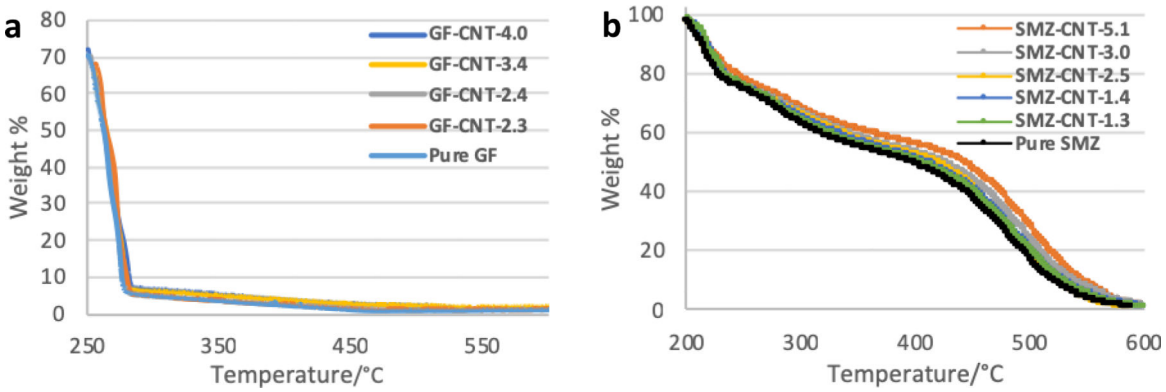

Figure 2.

TGA curve of drug and drug incorporated with different amount of f-CNTs: (a) GF-CNT and (b) SMZ-CNT.

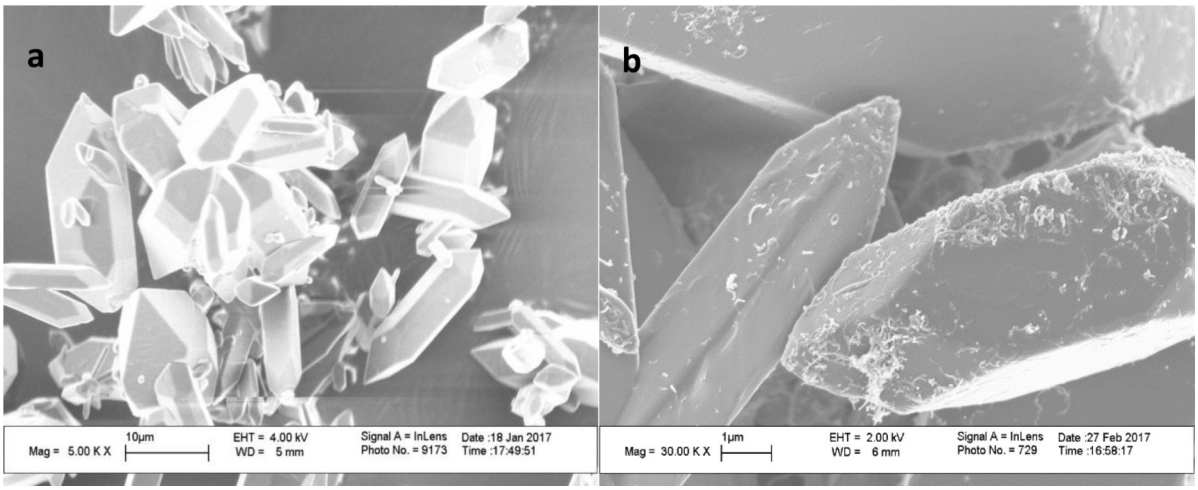

Figure 3.
SEM images of (a) Pure GF and (b) GF-CNT-2.4

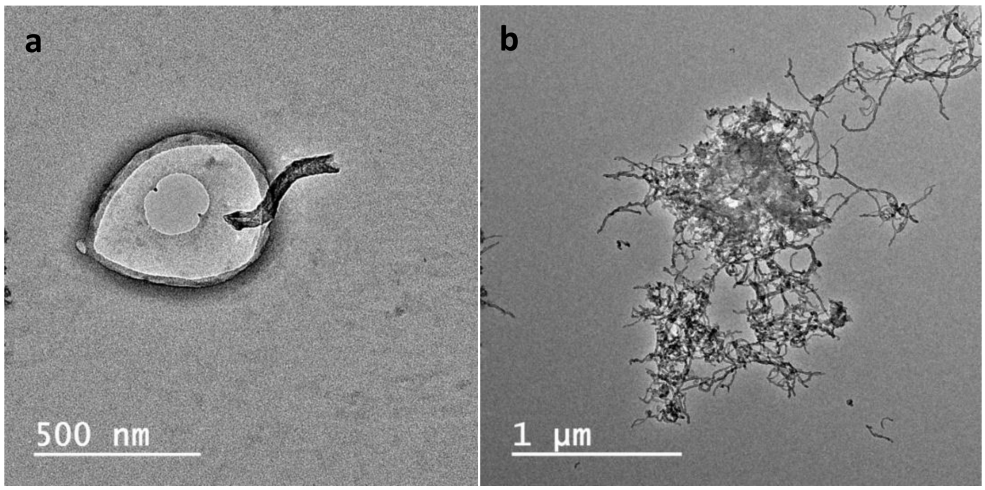

Figure 4.
TEM images of (a) GF-CNT-4.0 and (b) GF-CNT-2.7

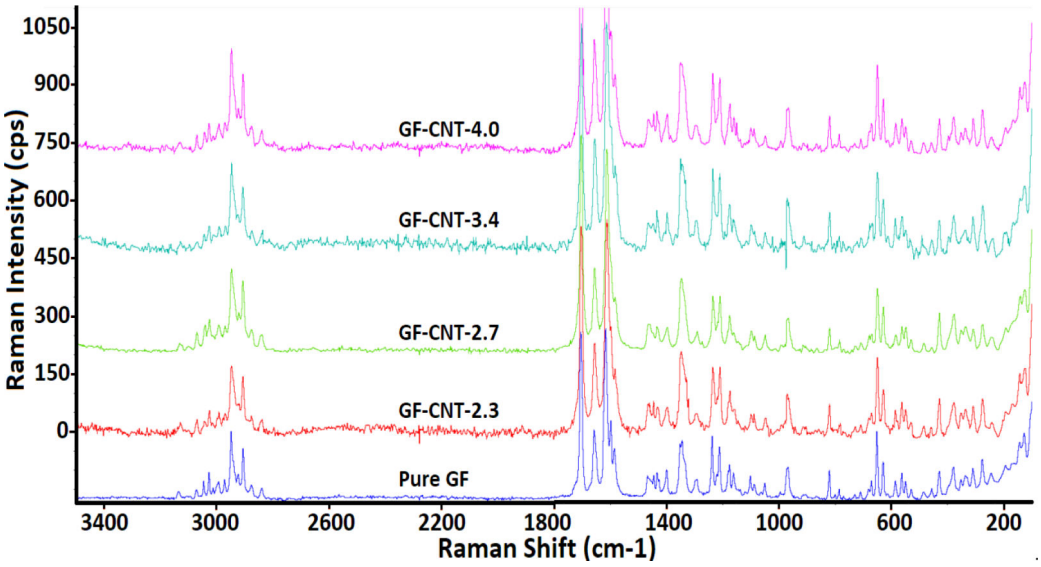

Figure 5.
RAMAN spectra of pure GF and GF incorporated with different amount of f-CNTs.

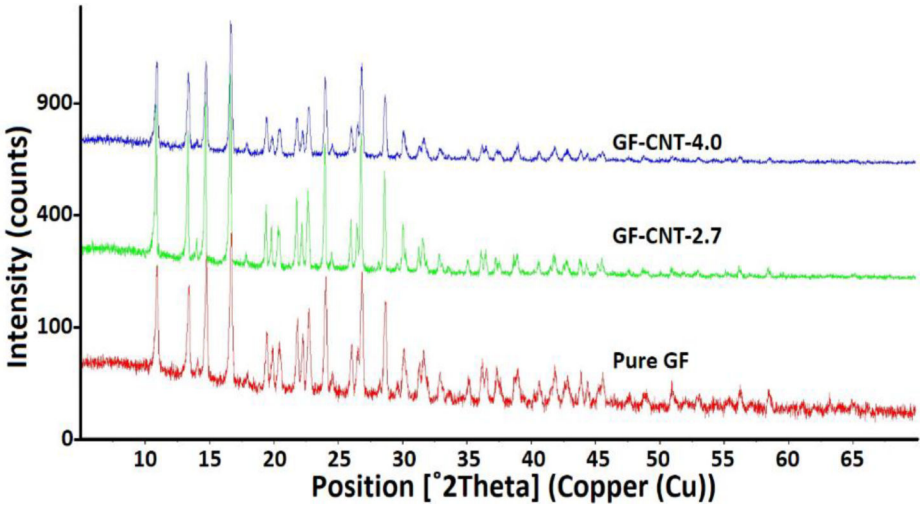

Figure 6.
XRD spectra of pure GF and GF incorporated with different amount of f-CNTs.

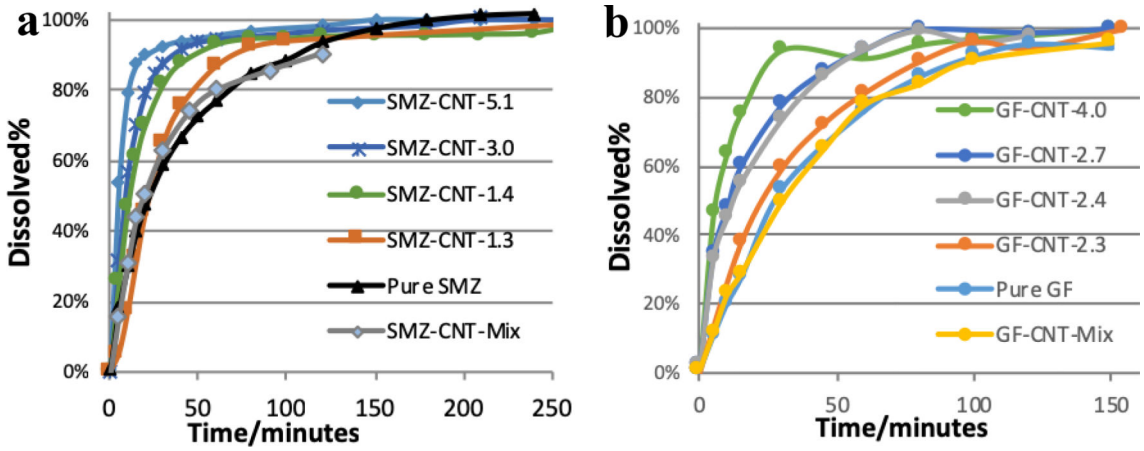

Figure 7.

Dissolution of (a) SMZ-CNTs and (b) GF-CNTs showed enhanced dissolution with the incorporation of f-CNTs in drug crystals.

Table 1.

Dissolution and melting point of SMZ-CNTs and GF-CNTs

	Amount of CNT in Composite (%)	T_{50} (min)	T_{80} (min)	M_p (°C)
SMZ	0	22	67	170.37
	1.3	20	38	170.31
	1.4	10	29	170
	3.0	8	21	170.38
	5.1	5	10	169.96
GF	0	27	66	221.25
	2.3	22	56	221.3
	2.4	12	48	221.08
	2.7	11	33	221.04
	4.0	6	18	220.38